

# Mapping the Moon: Using a lightweight AUV to survey the site of the 17th Century ship ‘La Lune’

Nuno Gracias\*, Pere Ridao\*, Rafael Garcia\*, Javier Escartín†, Michel L’Hour¶, Franca Cibecchini¶, Ricard Campos\*, Marc Carreras\*, David Ribas\*, Narcís Palomer\*, Lluís Magi\*, Albert Palomer\*, Tudor Nicosevici\*, Ricard Prados\*, Ramon Hegedüs‡, Laszlo Neumann¶, Francesco de Filippo§, Angelos Mallios\*

\* Computer Vision and Robotics Group, University of Girona, Spain  
Emails: {ngracias, pere, rafa}@silver.udg.edu

† Équipe de Géosciences Marines, IPGP, Univ. Paris Diderot, France

‡ Max Planck Institute for Informatics, 66123 Saarbrücken, Germany,

§ Università della Calabria, Arcavacata di Rende, Italy,

¶ DRASSM, Marseille, France

|| ICREA, Barcelona, Spain

**Abstract**—This paper describes the use of a research-driven, highly reconfigurable autonomous underwater vehicle for surveying the site of the historical shipwreck of *La Lune*. This wreck, from the XVII century, lies in 90m of water near the coast of Toulon in France. The goal of this survey was to create a fast but detailed map of the site, to serve as a base map for subsequent archaeological intervention. The paper overviews the survey setup and the methods used to generate a high resolution optical map. It also highlights some of the important advantages that lightweight AUVs present for archaeological survey missions in terms of operational costs, survey time, the quality of both the acquired data and the mapping outcome, and access to deep sites that are not reachable by traditional archaeological methods.

## I. INTRODUCTION AND GOALS

Traditional underwater archaeology is generally performed via SCUBA diving but is constrained by the practical depth that a diver can work (normally limited to 50 meters) and the time that can be spent underwater. New technologies, like manned submersibles, remotely operated vehicles (ROVs) and more recently autonomous underwater vehicles (AUVs) allow archaeologists to survey at depths up to 6000m, which corresponds to 98% of the world’s ocean seafloor. This increases dramatically the number of underwater sites available for archaeological study.

Although technology plays a significant part in this work, it needs to be combined with the research methodologies used by archaeologists, so that archaeology in deep water conforms to the required standards [1]. Over the last few years it has been clearly demonstrated that archaeologists can benefit from new underwater technology but their requirements pose new and sometimes fundamental problems for engineers [2], such as the need for very accurate navigation and mapping quality.

Manned submersibles have the unique advantage of allowing scientists to physically reach the deep and perform systematic observation on sites of particular interest as well as recovering artifacts [3]. However, because of their operational costs and complexity, their availability is very limited. An important step forward towards deep water archaeology came

from the use of ROVs. With continuous power supply from the deployment ship, they can support a wide range of sensors, uninterrupted operations and can recover artifacts with heavy but precise manipulators [4], [5], [6]. ROVs are generally powered and controlled from a tether cable. This provides unlimited autonomy in terms of power and time, but limits the range and mobility of the vehicles. Furthermore the deeper the operations are, the higher the deployment and usage costs tend to be (e.g. larger support ship, and shiptime dedicated exclusively for ROV tracking).

Although limited in power, AUVs alleviate some of the drawbacks of ROVs. By avoiding the tether management constraints, AUVs can improve the efficiency of archaeological surveys and decrease the operational costs. Understandably, there has been a sharp increase on the use of AUVs over the last decade, for both commercial and scientific applications.

Early uses of AUVs in marine archaeology are reported in [7]. In 2004, Meo [8] discusses the applications of new technologies in the study of underwater archeological sites, emphasizing the advantages of AUVs in such scenarios. Foley et al. [9] provide a detailed description of the archaeological study of two 2000 years old ships. Due to the depth of the sites (70m) the use of divers was not practical. As an alternative, the research team successfully used AUV systems to map and study the sites. An extensive review of the AUVs usage and deepwater archaeological techniques can be found in [2], [10].

This paper presents the survey setup and initial results of a recent (2012) survey of a shipwreck off the Mediterranean French coast. For this work we used the Girona 500 AUV, which was recently developed by the University of Girona.

The *La Lune* was a three-masted, 38m long vessel, and was part of the fleet of King Louis XIVs (Fig. 1). It was lost soon after returning from the North of Africa, on November 6th 1664, with 350 sailors and at least 450 soldiers aboard. The ship had returned already in poor condition from a campaign in Djidjelli, nowadays part of Algeria [11]. Upon arriving to France it was hastily refitted, so that it could be promptly used

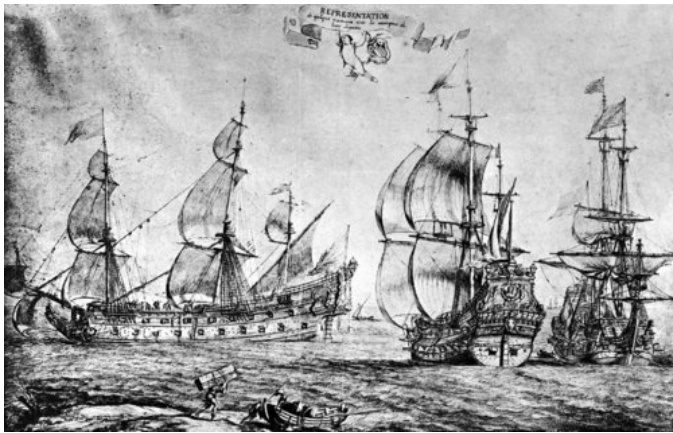


Fig. 1. The only known representation of the 'La Lune' (first ship on the left), from a 1690 painting. (©Musée National de la Marine, S. Dondain, France).

to carry a large amount of people from Toulon to the nearby island of Porquerolles for quarantine. The ship started taking in water shortly after leaving to port of Toulon, and eventually broke in two pieces, only a few miles from coast. The breaking and sinking happened in quick succession, which contributed to the large number of casualties[11]. More than 700 people perished in the accident.

The wreck was discovered accidentally in the spring of 1993 during a test trial of the IFREMER submarine *Nautilie* [12]. Soon after its discovery, the wreck site was assessed by the french Département des Recherches Archéologiques Subaquatiques et Sous-Marines (DRASSM), using an ROV [13]. Upon conclusion of that initial archaeological survey, the wreck was classified as one of the best preserved of its kind in the world. The site is considered as an experimental laboratory for the development and testing of new extraction methods for deep-water archeology [14].

In early 2012 the site was mapped using a Kongsberg Maritime EM2040 multibeam echosounder, deployed from the AsterX AUV [15]. These data allowed for obtaining a detailed bathymetry of the site, with a spatial cell resolution of 10 cm.

Subsequently, the site was optically surveyed in August 2012 with the Girona 500 AUV. The main objective was the creation of a preliminary optical cartography of the site, to serve as the base map for posterior archeological intervention, that took place a few weeks after. This mapping work is also integrated within the preparation of a television documentary, currently in production.

## II. SURVEY SETUP

The Girona 500 (Fig. 2) is a compact-size AUV designed for a maximum operating depth of 500m [16]. The vehicle is built around an aluminum frame which supports three torpedo-shaped hulls and other elements such as the thrusters. The overall dimensions of the vehicle are 1m in height, 1m in width, 1.5m in length and a weight (on its basic configuration) of about 140kg. The two upper hulls, which contain the flotation foam and the electronics housing, are positively buoyant, while the lower one contains the heavier elements such as the batteries and the payload. This particular arrangement of the

components provides the vehicle with passive stability in pitch and roll, making it suitable for tasks requiring a stable platform such as video surveying or intervention.

An important characteristic of the Girona 500 is its capacity to reconfigure for different tasks. In its basic configuration, the vehicle is equipped with typical navigation sensors (DVL, AHRS, pressure gauge and USBL) and basic survey equipment (profiler sonar, side scan sonar, video camera and sound velocity sensor). In addition to these sensors, almost half the volume of the lower hull is reserved for mission-specific payloads. This allows the modification of its sensing and actuation capabilities as required. A similar philosophy has been applied to the propulsion system which can be set to operate with a different number of thrusters, ranging from 3 to 8, to actuate the necessary degrees of freedom and provide redundancy, if required.

The Girona 500 AUV is the principal outcome of the Spanish funded RAUVI project, whose aim was to setup a low-cost, light-weight Intervention Autonomous Underwater Vehicle (I-AUV). In 2011, an autonomous object search and recovery task was demonstrated in a water-tank using a 4DOF electrical-driven arm mounted in the payload area [17]. The robot was launched first, to conduct an optical survey. Next, a photomosaic of the surveyed area was assembled offline, allowing a user to select the target object. Then, the robot was launched again to autonomously hook the target object. In the context of the TRIDENT FP7 project, the I-AUV was upgraded and the experiment was reproduced at sea, in more realistic conditions in a harbor environment [18]. Recently, in October 2012, a 7 DOF arm equipped with a 3 finger hand was integrated in the vehicle and the object search and recovery task was reproduced using free-floating manipulation techniques. The first science-oriented cruise took place in July 2012, within the Eurofleets CALDERA 2012 project. The cruise objectives included the operational validation of Girona 500 for field science applications [19]. During this cruise the robot dived to the bottom of the Santorini Caldera to a maximum depth of 380 m to collect video and multi-beam data.

For the *La Lune*, the AUV was equipped with a recently developed high-resolution stereo imaging system (Fig. 3). The main part of the system is a 500m rated cylindrical pressure housing made from hard-anodized aluminum alloy and with two rectangular viewports made of highly transparent polymethyl methacrylate (PMMA). The cylinder contains two Canon EOS 5D Mark II still cameras, with 21MPixel sensors and Canon 24mm lenses. The cameras are connected to a PC-104 computer stack which can store and post-process the images if necessary. The computer is also in charge of controlling and logging data from an echosounder whose transducer is mounted between the two viewports (Fig. 3, right). The echosounder ranging assists the focusing of the cameras. This mechanism is helpful under mild image turbidity, as the cameras are not required to do optical-based focusing. The housing has several connectors which make possible to interface with the Girona 500, to connect with auxiliary systems such as an external multibeam echosounder and to control the lighting system. The lighting system comprises four 40W LED lamps, which can operate either in continuous or in strobe mode. The imaging and lighting systems were mounted in the free payload

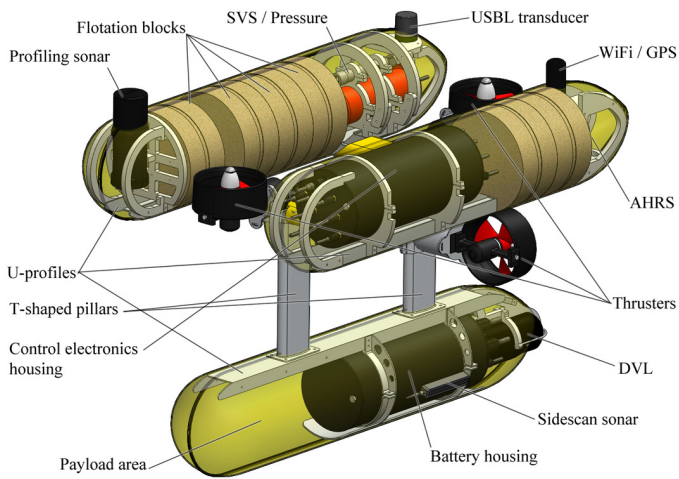


Fig. 2. Schema of the Girona 500 AUV, showing the location of principal components and payload area.



Fig. 3. High resolution stereo imaging system.

area of the AUV (Fig. 5).

### III. DATA ACQUISITION AND PROCESSING

The Girona 500 AUV was deployed from the R/V *Bon Pigall* (Spain). This 24m vessel illustrates an important advantage of low-weight AUVs, which can be deployed from small ships. Although the R/V *Bon Pigall* is equipped with dynamic positioning, it was not required for AUV operations. Also, the ship's 200kg crane was sufficient for the deployments and recoveries of the AUV (Fig. 4).

The data were collected in two consecutive dives of one hour each. At the nominal survey altitude of 3.68 meters, the imaging setup leads to a pixel footprint of 0.66mm. Such high ground resolution enables accurate artifact interpretation while allowing for a safe navigation clearance from the bottom.

The total bottom time was 103 mins. In this period, 2757 stereo image pairs were collected at a rate of 0.5 frames/s. The nominal forward speed of the vehicle was 0.5 m/s. At the prescribed altitude above the seafloor, the forward speed induced an overlap in the range of 50%–60% among time consecutive images (for each camera).

Part of the data collected during the survey were used to rapidly produce a highly detailed optical base map of the whole site. This map was created using an offline, batch optimization approach based on monocular image registration in 2D. While the site possesses objects with distinctive 3D content such as obliquely standing cannons and large vases, a large percentage of the site lies on a flat slope.



Fig. 4. The lightweight AUV GIRONA500 being deployed from the 24m R/V *Bon Pigall* above the *La Lune* shipwreck.

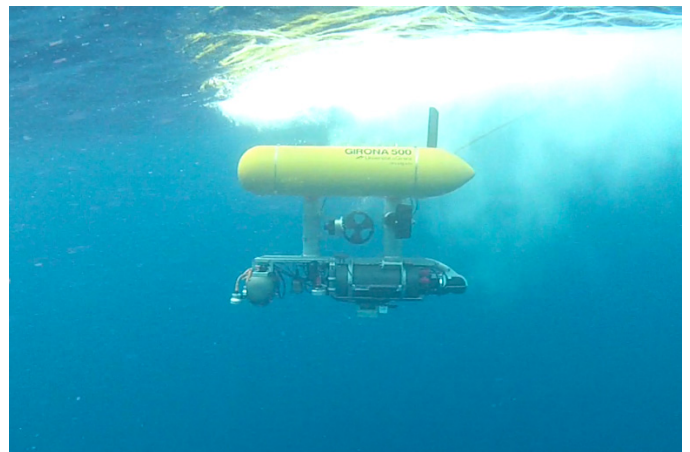


Fig. 5. The Girona500 AUV at the surface. The stereo DSLR camera setup is visible at the front of the AUV, in the lower left.

The vehicle navigation data can be directly used to create a preview of the optical mosaic. This preview is based on defining a mapping between the original images and a mosaic frame using the position and orientation information provided by the vehicle sensors. The navigation data are not accurate enough to provide a good alignment of the images. However, this initial approximation may be useful to get a global view of the area in a very short time, to extract preliminary conclusions and to plan further missions on-site to insure adequate coverage of the site. Due to a sensor configuration issue during survey, the real-time navigation data were affected by unexpectedly large errors. Since a complete acoustic near-bottom bathymetry was available at the time [15], this bathymetry was used in the map creation process, to provide fiducial points. The fiducial points serve two purposes: (1) reduce geometric distortions on the mosaic and (2) allow its georeferencing.

The map creation process encompasses the following steps: (A) image preprocessing for the correction of lens distortion, uneven illumination and loss of contrast [20]; (B) feature based pairwise image matching; (C) Global alignment [21], (D) Image blending and texture draping, over the acoustic

bathymetric data previously collected by IFREMER [15].

### A. Preprocessing

Underwater imagery suffers from image degradation due to strong light scattering and absorption, presenting a challenge for underwater vision systems, for which none of the existing standard image processing methods provide a convincing solution. However, there are the so-called dehazing techniques, which aim at enhancing images affected by participating media. There is a group of such methods which rely on additional measurements to gather depth information, either by using polarization filters [22], capturing multiple images under different conditions [23], [24], or by registering the given hazy scene with already existing georeferenced digital terrain [25]. In contrast, they are the so-called single-image dehazing methods, which only utilize the inherent information within the recorded image to generate its enhanced version. In underwater scenarios Carlevaris-Bianco et al. [26]. applied a single image dehazing based on a Bayesian approach, while Chiang and Chen [27] based their approach on an image formation model with wavelength compensation. Adopting also a single image dehazing approach, for our purposes we have developed a versatile imaging framework that can handle underwater image restoration based on the algorithms found in [28] and [29]. Our robust dehazing tool is capable of significantly increasing the level of detail, enhancing the features seen in underwater photo-mosaics, some of them which would otherwise left unnoticeable even by expert archaeologists who are used to analyzing underwater imagery. The application of this processing to a sample image from the survey can be seen in Fig. 6.

### B. Pairwise image matching

The objective of this step is to find the relative displacement between pairs of overlapping images. Since these pairs are not known *a priori*, prospective image pairs are selected based on their temporal and spatial proximity. The spatial proximity is evaluated from the navigation data. If the navigation data is too unreliable or inexistent, the prospective pairs are selected using a fast texture similarity test [30, p. 63].

Each prospective image pair is attempted to be matched by detecting SIFT [31] features and descriptors on both images, followed by robust motion estimation using an homography as the motion model [21].

### C. Global alignment

The global alignment step estimates the location of all images on a common reference frame. It takes into account the correspondences among matched image pairs, and the available fiducial points. The following cost function is minimized:

$$\operatorname{argmin} \left( \tau \cdot \sum_{\substack{1 \leq l \leq m \\ 1 \leq k \leq n}} (\|i r_k^l\|^2 + \|j r_k^l\|^2) + \lambda \cdot \sum_{k=1}^o \|p r_k\|^2 \right) \quad (1)$$

where  $\tau$  and  $\lambda$  are relative weights,  $m$  is the number of correspondences between a given image pair,  $n$  is the number of image pairs with overlap and  $i r_k^l$ ,  $j r_k^l$  and  $p r_k$  are defined as follows:



(a)



(b)

Fig. 6. Original survey image containing part of two canons (a) and its illumination corrected, de-hazed version (b).

$$i r_k^l = i x_k^l - j^i H \cdot j \tilde{x}_k^l \quad (2)$$

$$j r_k^l = j x_k^l - i^j H \cdot i \tilde{x}_k^l \quad (3)$$

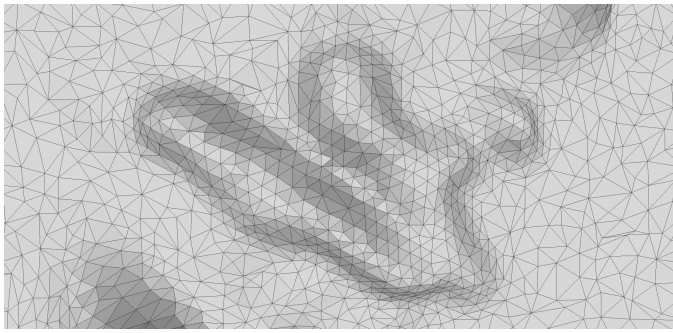
$$p r_k = i x_k - m^i H \cdot m \tilde{x}_{0k} \quad (4)$$

The first sum in Equation 1 represents the reprojection error of the correspondences, that is, the error which measures the distance between the result of applying the transformation to the interest points and the real point positions in both directions of the transformation. In Equation 2,  $i x_k^l$  is a point in image  $i$  while  $j \tilde{x}_k^l$  is its correspondence in image  $j$ . Both points are represented in homogeneous coordinates, and  $j^i H$  represents the planar transformation between both images, and is parametrized by 6 pose parameters that are being estimated. The roles are inverted in Equation 3.

The second sum in Equation 1 measures the deviation in the position from a given fiducial point  $i x_k$ , found in image  $i$ , with respect to the real position  $m \tilde{x}_{0k}$  in the mosaic plane.

### D. Blending and texture mapping

Image blending techniques combine the textures of multiple registered and overlapping images to create a single



(a)



(b)

Fig. 7. Close-up of two cannons from the bathymetry after Laplacian smoothing and decimation. (a) The mesh of triangles, (b) the same area with the draped mosaic.

mosaic. These techniques reduce the visibility of the seams along the borders of neighboring images, and provide an uniform appearance to all regions of the mosaic. The used methods are described in [20], [32].

After applying standard cleaning and processing of raw multibeam data, the bathymetry is represented on a regular grid, with depth values for each element. To transform grid into a virtual 3D model, the gridded depths were triangulated. The most straightforward approach is to break each grid element into two triangles. Depending on the accuracy of the bathymetry, the resulting model may be noisy. Therefore a Laplacian smoothing method [33] was applied to the triangle mesh. At each iteration of the process, a vertex is moved to the mean position described by its neighbors and itself. The iteration is applied  $n$  times until the desired smoothing is achieved.

Depending on the resolution of the grid, the process of splitting each pixel into two triangles could lead to a sizable amount of triangles. However, the underlying geometry represented in the bathymetry can be represented faithfully using fewer triangles. For example, flat (or almost flat) areas of the model should be represented with fewer triangles than the more informative areas of high curvature. For this reason, the quadric error metrics decimation procedure [34] was applied. This method offers a good tradeoff between geometric accuracy and computational cost.

#### E. Mapping results

The optical base map was created from 845 images. These images were selected to be inside a bounding box of 80 by 50m

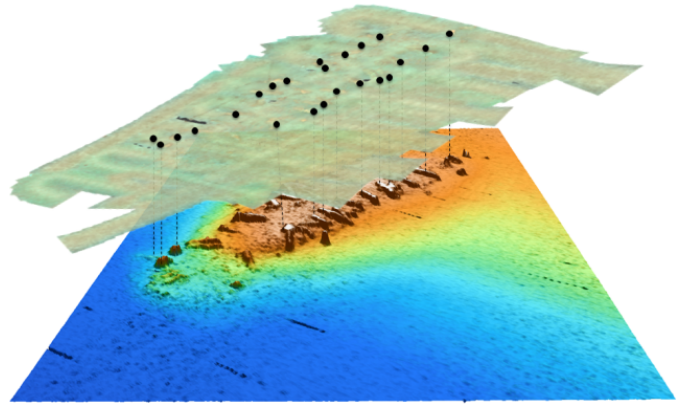


Fig. 8. Acoustic bathymetry used to provide ground control points.

defined over the location of site. A total of 23 fiducial points were obtained from the acoustic bathymetry. The points were chosen to be laying on structures that were easily recognizable in the original images and on the elevation map. The acoustic bathymetry and the used points are represented in Fig. 8.

The resulting optical map is shown in Fig. 9. In this north-up view, the ship centerline is easily recognizable by both the two lines of outward looking cannons, and by a marker line that was attached and left during a previous archaeological survey. The bulk of the artifacts are located within a well defined area of 65 by 20m, oriented along the center line. This area is shown in figure 10.

Since the optical map and the bathymetry are co-registered, it is straightforward to obtain a 2.5D textured model, by draping the mosaic over the elevation map, as seen on Fig. 11.

Ongoing work focuses on obtaining a full 3D reconstruction of the site, using multi-view stereo, navigation data and ground control points [35], [36], [37] together with the estimation of the uncertainty bounds of the 3D structures. The characterization of this uncertainty is essential to ensure compliance with the strict photogrammetric accuracy requirements needed for archaeological work.

A preliminary example of a 3D reconstruction from optical sensing only, is given in Fig. 12. For this model, a sequential structure-from-motion system [36] was used to obtain the camera trajectory. Then, a greedy dense multi-view stereo method retrieved a point set representing the object [38]. From this representation, the surface was extracted in the form of a triangle mesh using a reconstruction method [39], [37]. Finally, texture mapping was applied to the resulting model using the texture from the original images.

## IV. CONCLUSIONS

This ongoing work highlights some of the important advantages that light-weight AUVs present for archeology survey missions in terms of operational costs, survey time, and the quality of both the acquired data and the mapping outcome. Marine archeology traditionally relies on SCUBA diving which is restricted to 50m depth, thus leaving 98% of the seafloor out of reach. Deeper coastal waters hold a vast number of

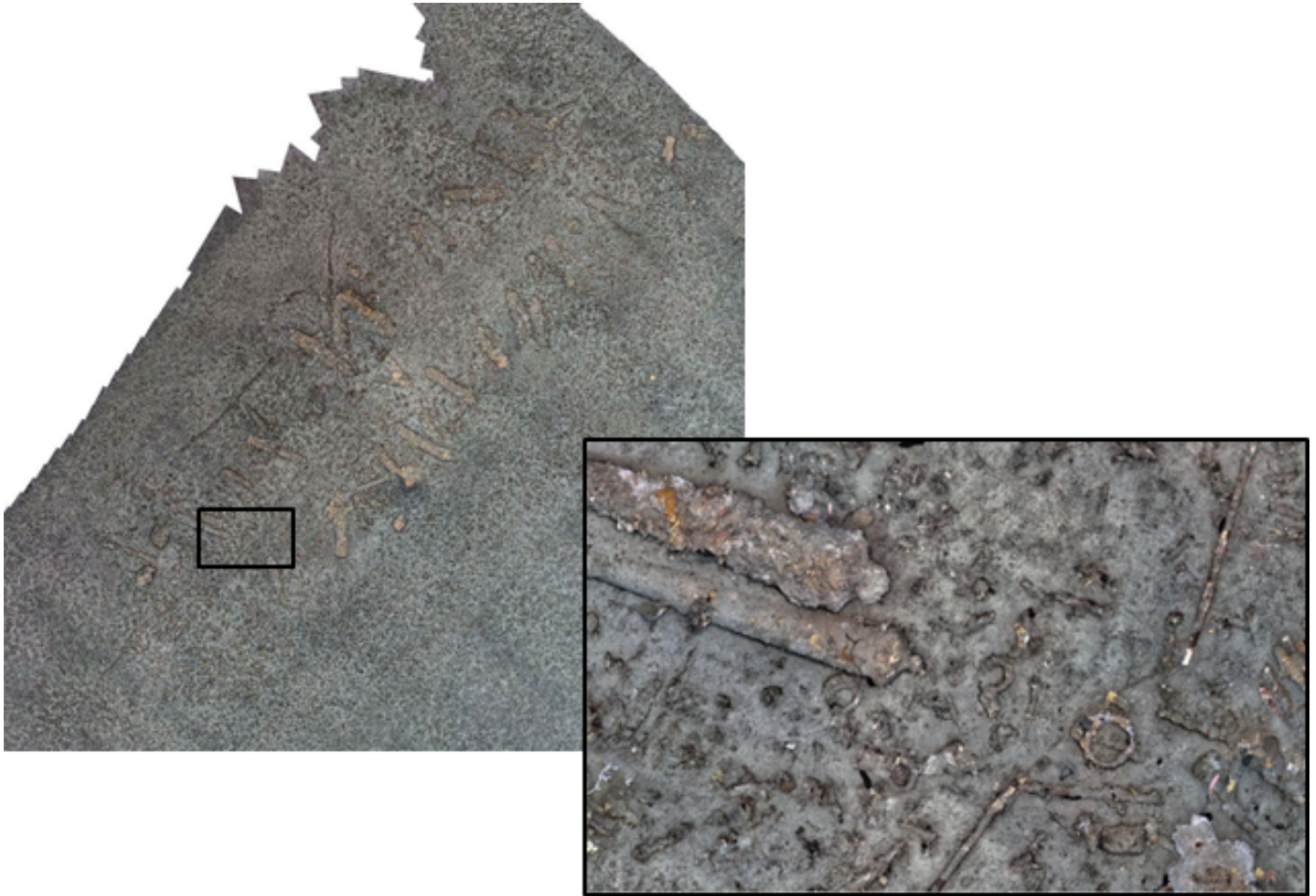


Fig. 9. Final optical map of the surveyed area (left), with zoomed-in inset (right). The inset covers an area of 15 by 8m, and illustrates the visual detail of the mosaic.

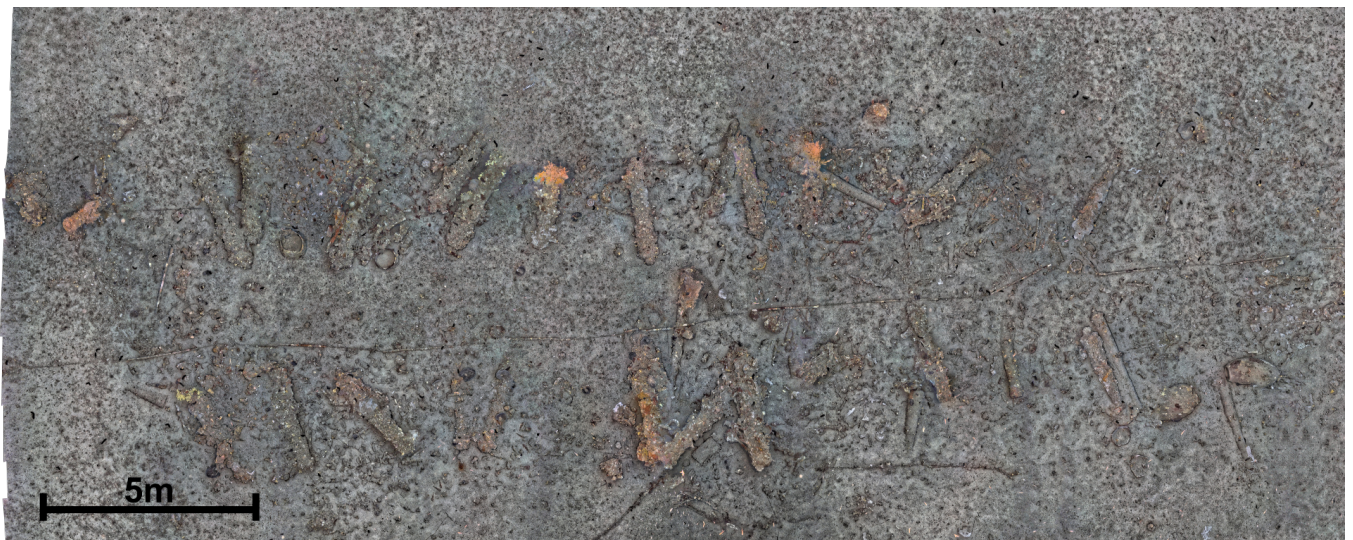


Fig. 10. Basemap photomosaic of the ship wreck rendered at 2.5mm/pixel. The ship centerline is marked by a line deployed during a previous archaeological survey [13]

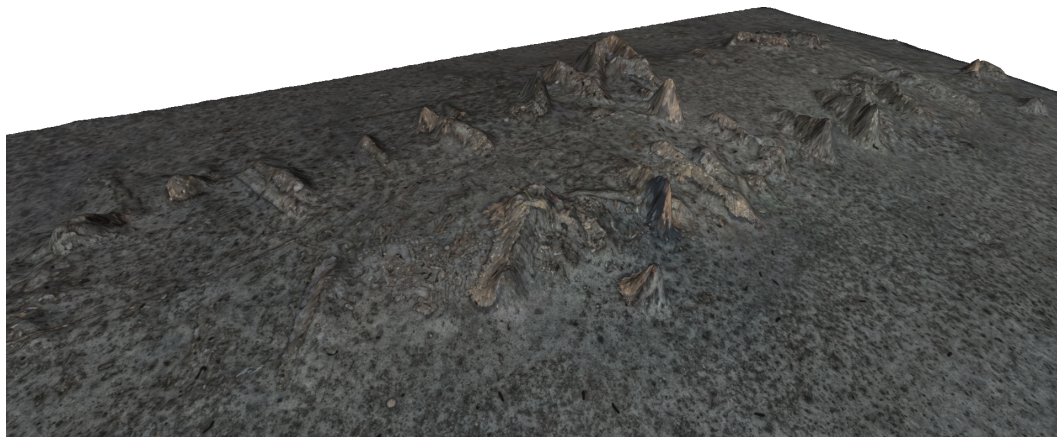


Fig. 11. Multimodal map combining the optical mosaic draped on top of the acoustic bathymetry.



Fig. 12. 3D reconstruction of a small area on the lower right of 10.

shipwrecks which tend to have little marine growth on them [9]. To reach deeper water, archeologists rely on ROVs or manned submersibles, which enable relatively fast mapping and surveying and intervention. However those systems have several shortcomings in terms of cost and human risk. A main factor driving up the cost is the need of dynamic positioning ships to support the vehicle operations, which may cost \$40K to \$100K USD per day [9] at present day prices.

Lightweight AUVs, like the one used in this work, can overcome some of these problems, and are expected to play an increasingly larger role in marine archeology in the near future.

#### ACKNOWLEDGMENTS

This work was partially funded by the Spanish MICINN under grants CTM2010-15216 (MuMap) and DPI2011-27977-C03-02 (COMAROB), the EU Project FP7-INFRASTRUCTURES-2012-312762 (EUROFLEETS2) and Marie Curie PERG-GA-2010-276778 (Surf3DSLAM). R. Campos was supported by the MICINN under the FPI program under grant CTM2010-15216. L. Newmann was supported by the Institució Catalana de Recerca i Estudis Avancats (ICREA). F. De Filippo was supported by the Project 'COMAS' (ref. PON01\_02140), financed by the MIUR under the PON 'R&C' 2007/2013 (D.D. Prot. n. 01/Ric. 18.1.2010). The

authors would like to thank the crew of the R/V *Bon Pigall* ([www.argomaris.com](http://www.argomaris.com)) and Pascal Guérin for their assistance during the survey.

#### REFERENCES

- [1] P. Holt, "An assessment of quality in underwater archaeological surveys using tape measurements," *International Journal of Nautical Archaeology*, vol. 32, no. 2, pp. 246–251, 2003.
- [2] B. Bingham, B. Foley, H. Singh, R. Camilli, K. Dellaporta, R. Eustice, A. Mallios, D. Mindell, C. Roman, and D. Sakellariou, "Robotic tools for deep water archaeology: Surveying an ancient shipwreck with an autonomous underwater vehicle," *Journal of Field Robotics*, vol. 27, pp. 702–717, 2010.
- [3] D. Sakellariou, P. Georgiou, A. Mallios, V. Kapsimalis, D. Kourkoumelis, P. Micha, T. Theodoulou, and K. Dellaporta, "Searching for ancient shipwrecks in the Aegean sea: the discovery of Chios and Kythnos hellenistic wrecks with the use of marine geological-geophysical methods," *International Journal of Nautical Archaeology*, vol. 36, no. 2.
- [4] R. Ballard, A. McCann, D. Yoerger, L. Whitcomb, D. Mindell, J. Oleson, H. Singh, B. Foley, J. Adams, D. Piechota, and C. Giangrande, "The discovery of ancient history in the deep sea using advanced deep submergence technology," *Deep Sea Research Part I: Oceanographic Research Papers*, vol. 47, no. 9, pp. 1591–1620, 2000.
- [5] B. Foley and D. Mindell, "Precision survey and archaeological methodology in deep water," *ENALIA: The Journal of the Hellenic Institute of Marine Archaeology*, vol. VI, pp. 49–56, 2002.
- [6] C. Roman, G. Inglis, and J. Rutter, "Application of structured light imaging for high resolution mapping of underwater archaeological sites," in *OCEANS 2010 IEEE - Sydney*, 2010, pp. 1–9.
- [7] D. Mindell and B. Bingham, "New archaeological uses of autonomous underwater vehicles," in *MTS/IEEE OCEANS Conference and Exhibition*, vol. 1, 2001, pp. 555–558.
- [8] G. Meo, "The HMI of an experimental underwater vehicle for archeological survey, inspection and remote touring of important submarine sites and finds," in *MTS/IEEE TECHNO-OCEANS Conference'04*, vol. 2, 2004, pp. 818–821.
- [9] B. Foley, D. Sakellariou, K. Dellaporta, B. Bingham, R. Camilli, R. Eustice, D. Evagelistis, V. Ferrini, M. Hansson, K. Katsaros, D. Kourkoumelis, A. Mallios, P. Micha, D. Mindell, C. Roman, H. Singh, D. Switzer, and T. Theodoulou, "New methods for underwater archaeology: The 2005 Chios ancient shipwreck survey," *Hesperia*, vol. 78, no. 2, pp. 269–305, 2009.
- [10] C. Roman and R. Mather, "Autonomous underwater vehicles as tools for deep-submergence archaeology," *Proceedings of the Institution of Mechanical Engineers, Part M: Journal of Engineering for the Maritime Environment*, vol. 224, pp. 327–340, 2010.
- [11] B. Bachelot, *Louis XIV en Algérie: Gigeri - 1664*. Editions L'Harmattan, Paris, 2011.

- [12] M. L'Hour, "The French Department of Underwater Archaeology: A brief overview," *Europ. Journal of Archaeology*, vol. 15, no. 2, pp. 275–284, 2012.
- [13] L. Long and A. Illouze, "'La Lune', un vaisseau de Louis XIV perdu en 1664 au large de Toulon. historique du naufrage et photogrammétrie de l'épave par 90 m de fond," *XIV Cahiers d'Archéologie Subaquatique*, vol. 14, p. 167, 2002.
- [14] Département des Recherches Archéologiques Subaquatiques et Sous-Marines (DRASSM), "Explore, protect, publicise and study humanity's drowned history," [http://www.culture.gouv.fr/culture/dp/archeo/pdf/drassm\\_brochure\\_uk\\_web.pdf](http://www.culture.gouv.fr/culture/dp/archeo/pdf/drassm_brochure_uk_web.pdf), 2012.
- [15] Institut Français de Recherche pour l'Exploitation de la Mer (IFREMER), "L'épave de La Lune, vieille de 350 ans, révélée au large de Toulon," [http://www.ifremer.fr/institut/content/download/58256/806608/file/12\\_04\\_17\\_CP\\_epave\\_LaLune.pdf](http://www.ifremer.fr/institut/content/download/58256/806608/file/12_04_17_CP_epave_LaLune.pdf), 2012.
- [16] D. Ribas, N. Palomeras, P. Ridao, M. Carreras, and A. Mallios, "Girona 500 AUV: From survey to intervention," *IEEE/ASME Transactions on Mechatronics*, vol. 17, no. 1, pp. 46–53, 2012.
- [17] M. Prats, D. Ribas, N. Palomeras, J. C. García, V. Nannen, S. Wirth, J. J. Fernández, J. P. Beltrán, R. Campos, P. Ridao, P. J. Sanz, G. Oliver, M. Carreras, N. Gracias, R. Marín, and A. Ortiz, "Reconfigurable AUV for intervention missions: a case study on underwater object recovery," *Intelligent Service Robotics*, vol. 5, no. 1, pp. 19–31, 2012.
- [18] M. Prats, J. Garcia, S. Wirth, D. Ribas, P. Sanz, P. Ridao, N. Gracias, and G. Oliver, "Multipurpose autonomous underwater intervention: A systems integration perspective," in *Control Automation (MED), 2012 20th Mediterranean Conference on*, 2012, pp. 1379–1384.
- [19] P. Nomikou, J. Escartín, P. Ridao, D. Sakellariou, R. Camilli, V. Ballu, M. Moreira, C. Mével, A. Mallios, C. Deplus, M. Andreani, O. Pot, R. Garcia, L. Rouzie, T. Gabsi, R. Campos, N. Gracias, . Hurtós, L. Magi, N. Palomeras, and D. Ribas, "Preliminary submarine monitoring of Santorini caldera: Hydrothermal activity, and seafloor deformation," Poster in *Volcanism of the Southern Aegean in the frame of the broader Mediterranean area 10-12*, October 2012.
- [20] R. Prados, R. Garcia, N. Gracias, J. Escartin, and L. Neumann, "A novel blending technique for underwater giga-mosaicing," *IEEE Journal of Oceanic Engineering*, vol. 37, no. 4, pp. 626–644, 2012.
- [21] J. Ferrer, A. Elibol, O. Delaunoy, N. Gracias, and R. Garcia, "Large-area photo-mosaics using global alignment and navigation data," in *Proceedings of the IEEE OCEANS Conference*, October 2007, pp. 1–9.
- [22] Y. Schechner, S. Narasimhan, and S. Nayar, "Instant dehazing of images using polarization," in *Computer Vision and Pattern Recognition, 2001. CVPR 2001. Proceedings of the 2001 IEEE Computer Society Conference on*, vol. 1, 2001, pp. I-325–I-332 vol.1.
- [23] F. Cozman and E. Krotkov, "Depth from scattering," in *Computer Vision and Pattern Recognition, 1997. Proceedings., 1997 IEEE Computer Society Conference on*, 1997, pp. 801–806.
- [24] S. G. Narasimhan and S. K. Nayar., "Interactice (de)weathering of an image using physical models," in *ICCV Workshop on Color and Photometric Methods in Comp. Vision.*, 2003.
- [25] J. Kopf, B. Neubert, B. Chen, M. Cohen, D. Cohen-Or, O. Deussen, M. Uyttendaele, and D. Lischinski, "Deep photo: model-based photograph enhancement and viewing," *ACM Trans. Graph.*, vol. 27, no. 5, pp. 116:1–116:10, Dec. 2008.
- [26] N. Carlevaris-Bianco, A. Mohan, and R. Eustice, "Initial results in underwater single image dehazing," in *OCEANS 2010*, 2010.
- [27] J. Y. Chiang and Y.-C. Chen, "Underwater image enhancement by wavelength compensation and dehazing," *IEEE Transactions on Image Processing*, vol. 21, no. 4, April 2012.
- [28] J. P. Tarel and N. Hautiere, "Fast visibility restoration from a single color or gray level image," in *Computer Vision, 2009 IEEE 12th International Conference on*, 2009, pp. 2201–2208.
- [29] H. Kaiming, S. Jian, and T. Xiaoou, "Guided image filtering," *IEEE Transactions on Pattern Analysis and Machine Intelligence*, vol. 99, no. PrePrints, p. 1, 2012.
- [30] A. Elibol, N. Gracias, and R. Garcia, *Efficient Topology Estimation for Large Scale Optical Mapping*, ser. Springer Tracts in Advanced Robotics. Springer, 2012, vol. 82.
- [31] D. G. Lowe, "Distinctive image features from scale-invariant keypoints," *Int. J. Comput. Vision*, vol. 60, no. 2, pp. 91–110, Nov. 2004.
- [32] N. Gracias, M. Mahoor, S. Negahdaripour, and A. Gleason, "Fast image blending using watersheds and graph cuts," *Image and Vision Computing*, vol. 27, no. 5, pp. 597–607, 2009.
- [33] G. Hansen, R. W. Douglass, and A. Zardecki, *Mesh Enhancement : Selected Elliptic Methods, Foundations and Applications*. London: Imperial College Press, 2005.
- [34] M. Garland and P. S. Heckbert, "Surface simplification using quadric error metrics," in *Proc. of SIGGRAPH '97*.
- [35] M. Johnson-Roberson, O. Pizarro, S. B. Williams, and I. Mahon, "Generation and visualization of large-scale three-dimensional reconstructions from underwater robotic surveys," *Journal of Field Robotics*, vol. 27, no. 1.
- [36] T. Nicosevici, N. Gracias, S. Negahdaripour, and R. Garcia, "Efficient three-dimensional scene modeling and mosaicing," *Journal of Field Robotics*, vol. 26, pp. 759–788, October 2009.
- [37] R. Campos, R. Garcia, and T. Nicosevici, "Surface reconstruction methods for the recovery of 3D models from underwater interest areas," in *OCEANS, 2011 IEEE - Spain*, 2011, pp. 1–10.
- [38] Y. Furukawa and J. Ponce, "Accurate, dense, and robust multi-view stereopsis," *IEEE Trans. on Pattern Analysis and Machine Intelligence*, vol. 32, pp. 1362–1376, 2010.
- [39] M. Kazhdan, M. Bolitho, and H. Hoppe, "Poisson surface reconstruction," in *Eurographics Symposium on Geometry Processing*, 2006, pp. 61–70.